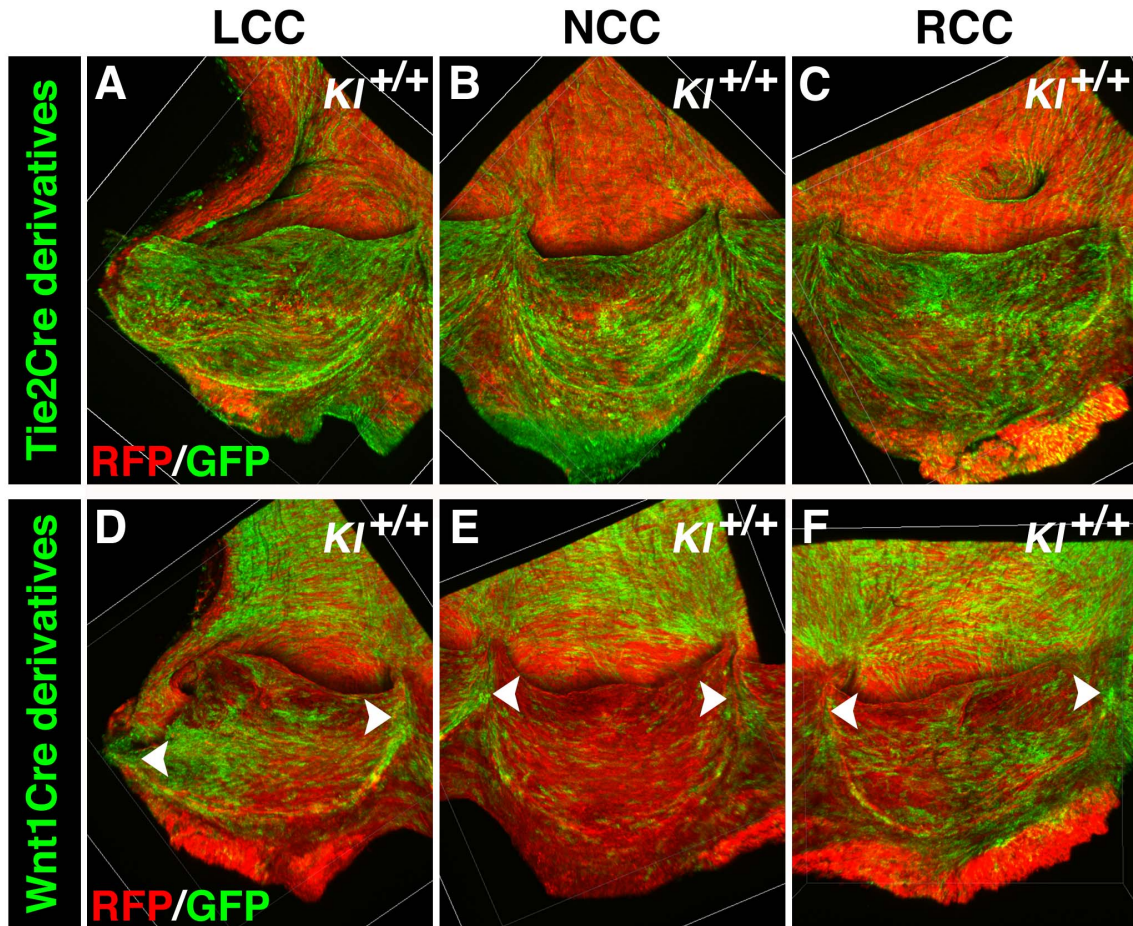
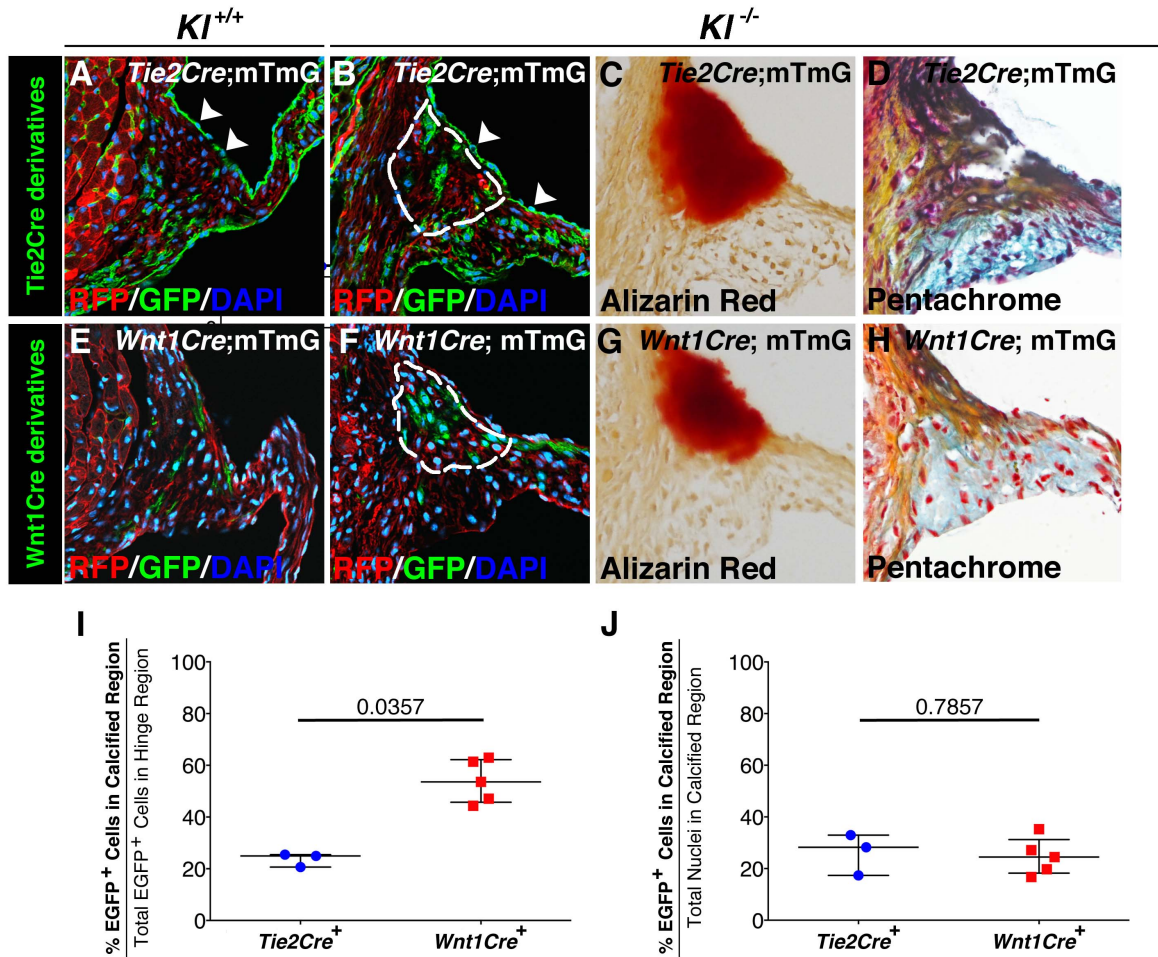


SUPPLEMENTARY MATERIAL
BMP Signaling is Required for Aortic Valve Calcification
(Gomez-Stallons et al.)

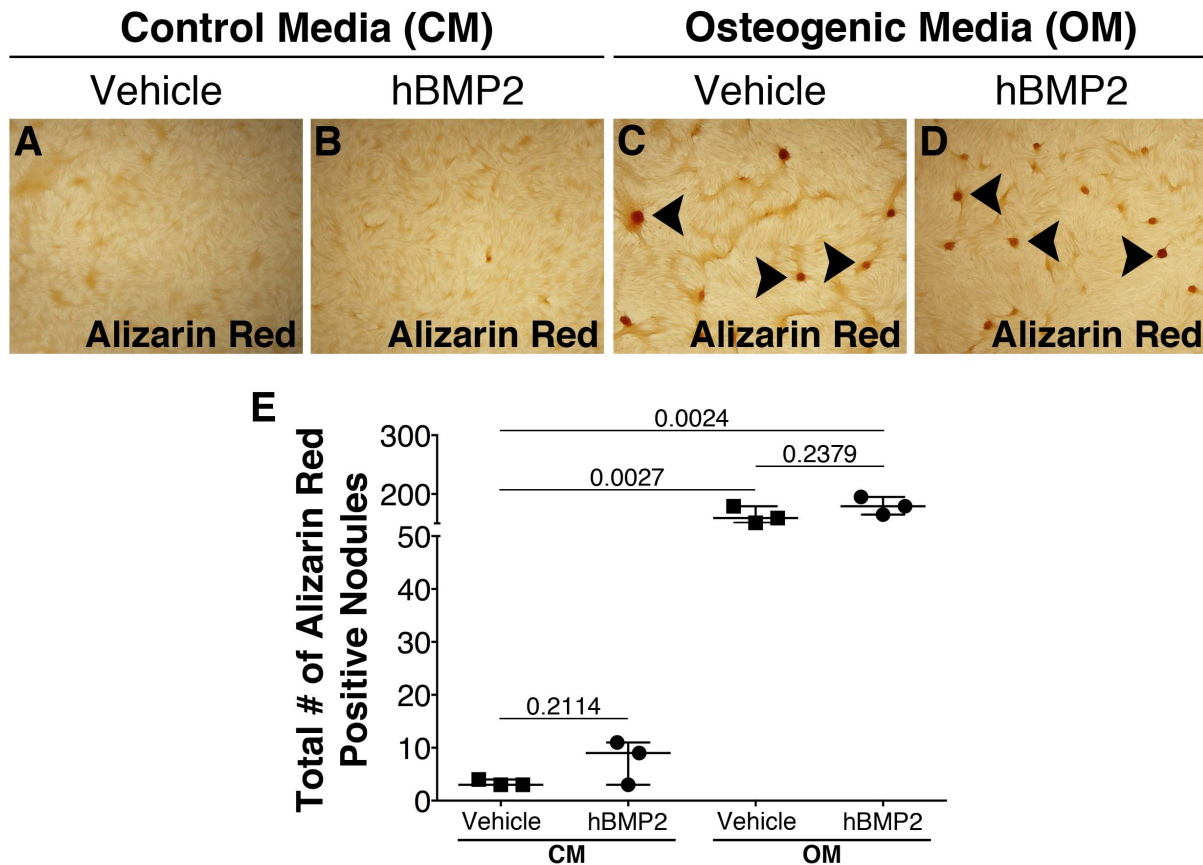


Supplementary Figure 1: Endothelial and neural crest derivatives are abundant in the AoV leaflets but display differential distribution. Lineage tracing studies in 6-week old wild type mice show endothelial-derived Tie2Cre (A-C) and neural crest-derived Wnt1Cre cells (D-F) in the aortic root, including AoV leaflets. *ROSA26^{mTmG}* reporter mice were used to trace Cre-recombined cells. Within the whole mount images, green fluorescence represents EGFP (GFP) expression, indicative of Cre-mediated recombination, while red tomato protein (RFP) fluorescence represents cells that do not express Cre-recombinase (A-F). Tie2Cre endothelial-derived cells (A-C, green fluorescence) are abundant in each of the three AoV leaflets and display even distribution among the leaflets. Wnt1Cre neural crest-derived cells (D-F, green fluorescence) are abundant in the AoV hinge region (white arrowheads). A total of 3 mice were analyzed for Tie2Cre cell derivatives (A-C). A total of 7 mice were analyzed for Wnt1Cre neural crest cell derivatives (D-F).

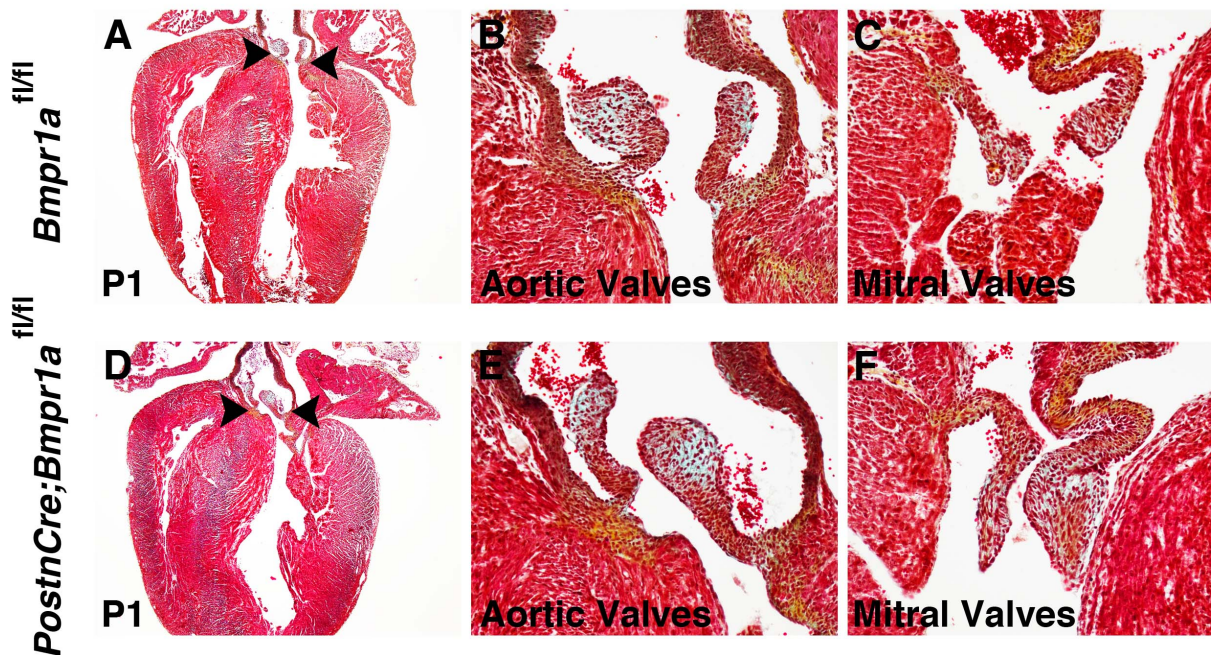


Supplementary Figure II: Wnt1Cre derivatives preferentially localize to regions of AoV calcification, compared to surrounding healthy valve tissue. *Tie2Cre;ROSA26^{mTmG}* and *Wnt1Cre;ROSA26^{mTmG}* mice were crossed with *Klotho*^{-/-} (*Kl*^{-/-}) mice to determine endothelial and neural crest contributions to calcified areas at 6 weeks. *Klotho*^{+/+} (*Kl*^{+/+}) mice were used as controls (A,D). Green fluorescence (GFP) represents EGFP expression, indicative of Cre-mediated recombination, while red tomato protein fluorescence (RFP) represents all cells that do not express Cre-recombinase (A-B, D-E). Nuclei are counterstained with DAPI (blue fluorescent cells (A-B, D-E). *Tie2Cre* endothelial-derived cells (GFP-positive cells) are distributed throughout the hinge regions of the valve leaflets (B-C). Surface endothelial cells were excluded from quantitative analysis (A,B, white arrowheads). In contrast, compared to surrounding valve hinge tissue, a greater percentage of *Wnt1Cre*-derived cells (GFP-positive cells) are observed in the calcified region (D-F). Calcified areas within the valve tissues were identified by Alizarin Red positive staining (red staining in C,F). Pentachrome staining shows ECM disruption in areas of calcification, but not associated with a specific lineage (D, H). A greater percentage of EGFP-positive *Wnt1Cre* derivatives were observed in the calcified valve regions (~60%), compared to surrounding healthy tissue, whereas *Tie2Cre* derivatives were evenly distributed throughout the hinge tissue (~20%) (I; $p = 0.0357$). Quantification of the number of EGFP-positive cells in the calcified regions of AoVs from *Kl*^{-/-};*Tie2Cre;ROSA26^{mTmG}* ($n=3$) and *Kl*^{-/-};*Wnt1Cre;ROSA26^{mTmG}* ($n=5$) mice did not reveal a difference in the number of cells from each lineage observed in the regions of calcification (J, $p = 0.7857$). Panel I displays

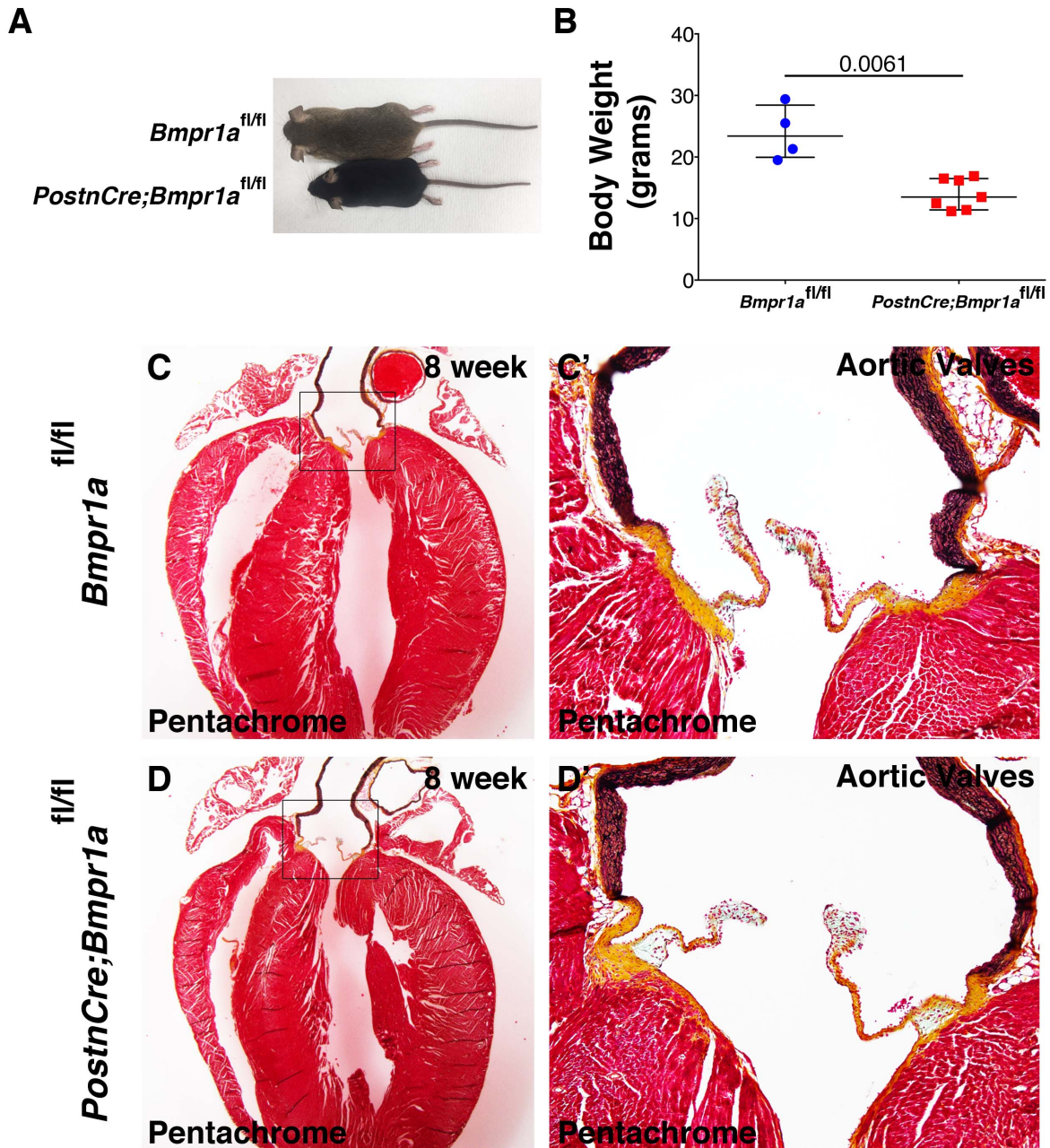
the percent (%) EGFP⁺ cells localized specifically to the calcified region (within the hinge region), compared to the total number of EGFP⁺ cells found at the hinge region (representing 100% of the cells). Panel J displays the total percent (%) contribution of EGFP⁺ cells to the calcified areas, compared to the total number of nuclei localized to the calcified areas (representing 100% of the cells). Error bars are shown as interquartile means and scatter plot. Statistical significance was determined by Mann-Whitney U-test ($p < 0.05$).



Supplementary Figure III: BMP2 treatment is not sufficient to promote calcification of porcine aortic VICs cultured *in vitro*. Alizarin Red staining was used to detect calcification of porcine aortic VICs cultured in Osteogenic Media (OM) and Control Media (CM) for 9 days, in the absence or presence of human BMP2 (A-D). Alizarin Red stained calcific nodules are present in OM-treated and OM + hBMP2 (Red staining in C-D, black arrowheads) VICs. The total number of calcific nodules for each treatment group, as detected by Alizarin Red staining, was quantified (E). hBMP2 alone is not sufficient to promote calcific nodule formation (B, E $p=0.2114$), as compared to a significant increase in the number of calcific nodules in OM-treated (C, E $p=0.0027$) and OM-treated in the presence of hBMP2 (D, E $p=0.0024$). However, there is no significant difference between OM-treated groups in the absence or presence of hBMP2 (C and D, $p=0.2379$). Displayed values represent individual independent experiments run in triplicate (E). Similar images and quantification values were obtained in 3 different independent experiments. Each dot is representative of the total number of calcific nodules quantified per well for each treatment group. Error bars are shown as interquartile means in the scatter plot. Statistical significance was determined using Mann-Whitney U-tests ($p < 0.05$).

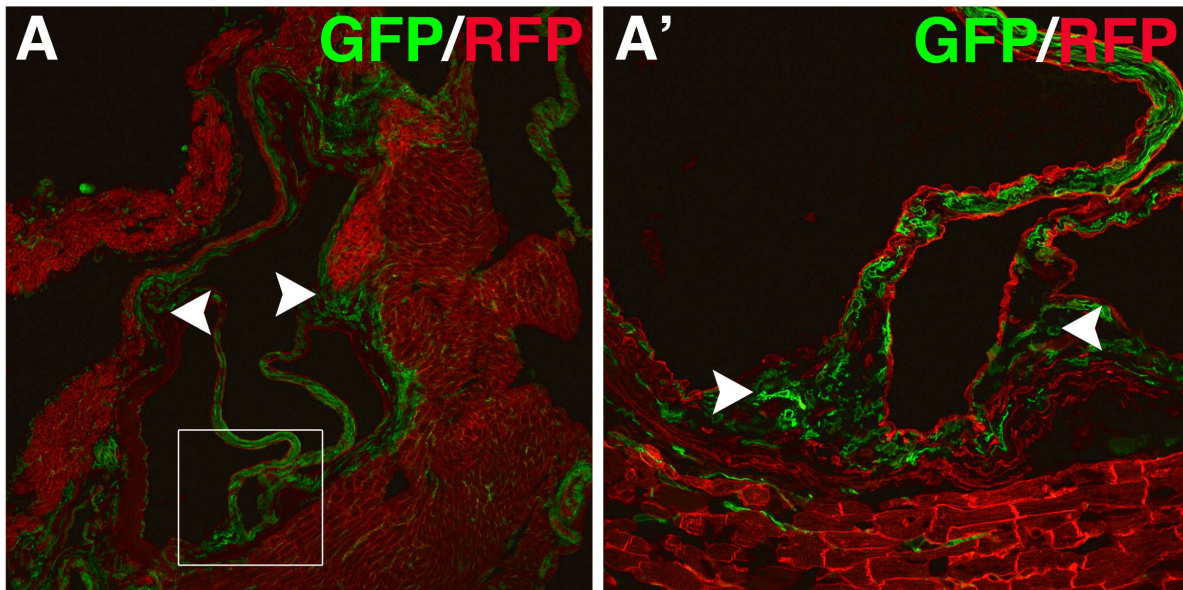


Supplementary Figure V: *PostnCre*-mediated genetic inactivation of the BMP receptor *Bmpr1a*/ALK3 does not lead to cardiac malformation in P1 mice. General heart and valve morphology was analyzed by Movat's Pentachrome staining in *Bmpr1a*^{fl/fl} (n=6) and *PostnCre; Bmpr1a*^{fl/fl} (n=6) mice at Post-natal day (P)1. Whole heart morphology depicting normal development in *PostnCre; Bmpr1a*^{fl/fl} (D) compared to control *Bmpr1a*^{fl/fl} P1 hearts (A). Normal AoV composition was observed in *PostnCre; Bmpr1a*^{fl/fl} and control *Bmpr1a*^{fl/fl} P1 mice (B,E show valves indicated by arrowheads in A,D). In addition, normal mitral valve composition was observed in *PostnCre; Bmpr1a*^{fl/fl} and control *Bmpr1a*^{fl/fl} P1 mice (C,F).



Supplementary Figure VI: Genetic inactivation of the BMP receptor *Bmpr1a*/ALK3 does not affect AoV maturation in adult mice. General body, heart and AoV morphology was analyzed in *Bmpr1a*^{fl^{ox}/fl^{ox}} (n=4) and *PostnCre; Bmpr1a*^{fl^{ox}/fl^{ox}} (n=7) 7-9 week old mice. Representative images of whole body anatomy of *PostnCre; Bmpr1a*^{fl^{ox}/fl^{ox}} adult mice compared to *Bmpr1a*^{fl^{ox}/fl^{ox}} controls is shown (A). As observed in Panel A and quantified in Panel B, *PostnCre; Bmpr1a*^{fl^{ox}/fl^{ox}} adult mice exhibit a significant decrease in body weight ($p=0.0061$). Movat's Pentachrome staining was used for analysis of whole heart morphology and AoV ECM composition of *PostnCre; Bmpr1a*^{fl^{ox}/fl^{ox}} (D, inset) compared to control *Bmpr1a*^{fl^{ox}/fl^{ox}} hearts at 2 months of age (C, inset).

$Kl^{-/-}; PostnCre; mTmG$



Supplementary Figure VII: *PostnCre*-mediated recombination occurs in VICs throughout the AoV of *Kltho*^{-/-} mice. *ROSA26*^{mTmG} reporter mice were used to trace *PostnCre*-mediated recombination in *Kltho*^{-/-}; *PostnCre*; *ROSA26*^{mTmG}. Cre-mediated recombination is detected by expression of green fluorescence (GFP), while red fluorescence (RFP) is detected in cells that do not express Cre-recombinase (A-A'). *PostnCre* expression in AoV of *Kltho*^{-/-} mice at 7 weeks of age is observed throughout the AoV, as seen in panel A (white arrowheads and inset). Panel A' shows robust expression of *PostnCre* at the hinge region of *Kltho*^{-/-} AoV (white arrowheads).

Supplementary Table IPrimer IDs for *Mus musculus* primer sets used for gene expression analysis.

Gene	Primer ID
<i>Aggrecan</i>	Mm00545794_m1
<i>Alkaline Phosphatase</i>	Mm00475834_m1
<i>B2m</i>	Mm00437762_m1
<i>BMP2</i>	Mm01340178_m1
<i>BMP4</i>	Mm00432087_m1
<i>Collagen I-a1</i>	Mm00801666_g
<i>Collagen II-a1</i>	Mm01309565_m1
<i>Collagen X-a1</i>	Mm00487041_m1
<i>Mef2c</i>	Mm01340842_m1
<i>Noggin</i>	Mm01297833_m1
<i>Osteocalcin</i>	Mm03413826_m1
<i>Osteopontin</i>	Mm00436767_m1
<i>Runx2</i>	Mm00501580_m1
<i>Smad6</i>	Mm00484738_m1
<i>Sox9</i>	Mm00448840_m1

Supplementary Table IIPrimer sequences for *Sus Scrofa* primer sets used for gene expression analysis.

Gene	Forward sequence	Reverse sequence
<i>18S</i>	5' TTGAAAATCCGGGGGAGAG 3'	5' ACATTGTTCCAACATGCCAG 3'
<i>BMP2</i>	5' CTCAGCGAGTTTGAGTTGCG 3'	5' TAAACTCCTCGGTGGGGACA 3'
<i>BMP4</i>	5' GCAAGTTTGTTTCAGGATTGGCT 3'	5' ACGACCATCAGCATTTCGGTT 3'
<i>Hapln1</i>	5' GGCGTCAGGAACTACGGTTT 3'	5' AACCGGCCATTGAAGTTGGA 3'
<i>Osteocalcin</i>	5' TCAACCCCGACTGCGACGAG 3'	5' TTGGAGCAGCTGGGATGATGG 3'
<i>Osteopontin</i>	5' TTGCTAAAGCCTGACCCATCT 3'	5' CGTCGTCCACATCGTCTGTT 3'